Image denoising and upscaling by means of four directions variational model

Alireza Hosseini

School of Mathematics, Statistics and Computer science, University of Tehran, P.O. Box 14115-175, Tehran, Iran
School of Mathematics, Institute for Research in Fundamental Sciences (IPM), P. O. Box: 19395-5746, Tehran, Iran
hosseini.alireza@ut.ac.ir

Abstract

In this paper, based on Condat's discrete total variation model, a modified discrete TV model is introduced for image processing problems. A dual formulation for the proposed TV is explained and an efficient primal-dual algorithm is employed to solve the problem. Some important image test problems are used in the numerical experiments. We compare our new model with state of the art models; isotropic, upwind, TGV and so on in image denoising and upscaling problems.

Keywords: image processing, variational methods, primal-dual optimization algorithm, upscaling, denoising

1. Introduction

In this paper a new variational model is proosed for solving image processing problems.
Assume $x \in (\mathbb{R})^{N_1 \times N_2}$, generally a mathematical image problem can be formulated by the following optimization problem:

$$\min \mathcal{F}(x) + \mathcal{R}(x). \tag{1}$$

where $\mathcal{F}$ represents the data fidelity and $\mathcal{R}$ is the regularization term. The most common fidelity term is of the form

$$\mathcal{F}(x) = \frac{1}{2}\|G(x) - g\|^2,$$

for appropriate function G and the given norm $\|.\|$. Most frequently chosen regularization term is given by

$$\mathcal{R}(x) = \lambda |x|^2,$$

where $|\ .\ |$ is Euclidean norm. Now, suppose $s : \Omega \subset \mathbb{R}^N \to \mathbb{R}$, $s \in L^1_{loc}(\Omega)$ is a locally Lipschitz, integrable N-dimensional function. Consider the following optimization problem to solve continuous version of mathematical image problems:

$$\min_s \frac{1}{2} \int_\Omega |G(s(t)) - g(t)|^2 dt + \lambda J(s), \tag{2}$$

where

$$J(s) = \sup \left\{ -\int_\Omega s.div\phi dt : \phi \in C^1_c(\Omega, \mathbb{R}^N), |\phi(t)| \leq 1, \forall t \in \Omega \right\}. \tag{3}$$

$J(s)$ is duality definition of total variation (TV) of the function s. A function s is said to have bounded variation whenever $J(s) < \infty$. The space $BV(\Omega)$ of functions with bounded variation is the set of functions $s \in L^1(\Omega)$ such that $J(s) < \infty$, endowed with the norm $\|s\|_{BV(\Omega)} = \|s\|_{L^1(\Omega)} + J(s)$. Obviously, for smooth function $s \in C^1(\Omega)$ (or $s \in W^{1,1}(\Omega)$),

$$J(s) = \int_\Omega |\nabla s| dt \tag{4}$$

For two dimensional smooth function s, minimization of $J(s)$ is equivalent to minimization of the majority of derivative over the dimension of the function. Intuitively, minimization problem (2) simultaneously tries to remove the noise from the continuous image s (which is equivalent to minimization of the total first derivative over the domain) and forces the function $G(s)$ to be near enough to g. See [12, 13, 15] and references therein.

2. The New discretization for total variation functional

In this section, a new discrete TV is introduced for solving image processing problems. Suppose $\Omega \subseteq \mathbb{R}^2$, $s \in L^1_{loc}(\Omega)$, $D_d s(t_1, t_2) = \frac{\partial s}{\partial t_1} + \frac{\partial s}{\partial t_2}$ and $D_e s(t_1, t_2) = \frac{\partial s}{\partial t_2} - \frac{\partial s}{\partial t_1}$ are directional derivatives of s at the directions of $d = (1, 1)$ and $e = (-1, 1)$ on (t_1, t_2) respectively. We can rewrite (4) as

$$J(s) = \int_\Omega |\nabla s| dt = \int_\Omega \sqrt{(\frac{\partial s}{\partial t_1})^2 + (\frac{\partial s}{\partial t_2})^2} dt_1 dt_2 = \frac{1}{\sqrt{3}} \int_\Omega \sqrt{(\frac{\partial s}{\partial t_1})^2 + (\frac{\partial s}{\partial t_2})^2 + (D_d s(t_1, t_2))^2 + (D_e s(t_1, t_2)^2} dt_1 dt_2. \tag{5}$$

For discrete image $x \in \mathbb{R}^{N_1 \times N_2}$, $(n_1, n_2) \in \{1, 2, \cdots, N_1\} \times \{1, 2, \cdots, N_2\} = X$, inspiring 5 and withdrawing coefficient $\frac{1}{\sqrt{3}}$, define the following predefined regularization semi-norm:

$$TV_{prn}(x) = \sum_{n_1=1}^{N_1} \sum_{n_2=1}^{N_2} \sqrt{((Dx)_1(n_1, n_2))^2 + ((Dx)_2(n_1, n_2))^2 + ((Dx)_3(n_1, n_2))^2 + ((Dx)_4(n_1, n_2))^2}, \tag{6}$$

where $(Dx)_1$ and $(Dx)_2$ are are forward difference operators and

$$\begin{aligned} D_d x(n_1, n_2) \approx (Dx)_3(n_1, n_2) = x(n_1 + 1, n_2 + 1) - x(n_1, n_2), \\ D_e x(n_1, n_2) \approx (Dx)_4(n_1, n_2) = x(n_1 - 1, n_2 + 1) - x(n_1, n_2), \end{aligned} \tag{7}$$

The equivalent definition of (6) is:

$$\begin{aligned} TV_{prn}(x) &= \max_{u=(u_1,u_2,u_3,u_4)\in(\mathbb{R}^4)^{N_1 \times N_2}} \{< \mathbb{D}x, u >: \ |u(n_1, n_2)| \leq 1, \ \forall (n_1, n_2) \in X\}, \\ &= \max_{u \in (\mathbb{R}^4)^{N_1 \times N_2}} \{- < x, \mathrm{div} u >: \ |u(n_1, n_2)| \leq 1, \ \forall (n_1, n_2) \in X\}. \end{aligned} \tag{8}$$

where $\mathbb{D}x = ((Dx)_1, (Dx)_2, (Dx)_3, (Dx)_4)^T$ and

$$|u(n_1, n_2)| = \sqrt{u_1^2(n_1, n_2) + u_2^2(n_1, n_2) + u_3^2(n_1, n_2) + u_4^2(n_1, n_2)} \tag{9}$$

and

$$\begin{aligned} \mathrm{div} u(n_1, n_2) = u_1(n_1, n_2) - u_1(n_1 - 1, n_2) + u_2(n_1, n_2) - u_2(n_1, n_2 - 1) \\ + u_3(n_1, n_2) - u_3(n_1 - 1, n_2 - 1) + u_4(n_1, n_2) - u_4(n_1 + 1, n_2 - 1). \end{aligned} \tag{10}$$

The second part of (8) corresponds to the original definition of total variation (3). Now we need to impose suitable boundary conditions on the image x and gradient field $u = (u_1, u_2, u_3, u_4)$, for which equalities in (8) is well defined.

2.1. Directional operators

Definition 2.1. : From now on, we use the following four indexes:
1. $\bullet$ is used for any element which is located in the center of a pixel. The location of an element v which is located in the center of pixel (n_1, n_2) is shown by (n_1, n_2) and we write $v \in A_\bullet$.
2. $\updownarrow$ is used for any element v which is located in the middle point of the edge which is the intersection of two pixels (n_1, n_2) and $(n_1 + 1, n_2)$ and thus the location of such element is on $(n_1 + \frac{1}{2}, n_2)$ and we write $v \in A_\updownarrow$.
3. $\leftrightarrow$ is used for any element v which is located in the middle point of the edge which is the intersection of two pixels (n_1, n_2) and $(n_1, n_2 + 1)$ and thus the location of such element is on $(n_1, n_2 + \frac{1}{2})$ and we write $v \in A_\leftrightarrow$.
4. $+$ is used for any element which is located in the vertex of a pixel. the element which is located in down right vertex of pixel (n_1, n_2) is located in $(n_1 + \frac{1}{2}, n_2 + \frac{1}{2})$ and we write $v \in A_+$.

Now we define three operators $L_{\updownarrow}, L_{\leftrightarrow}$, and $L_{\bullet}$ over $u \in (\mathbb{R}^4)^{N_1 \times N_2}$:

$$
\begin{aligned}
&(L_{\updownarrow}u)_1(n_1,n_2) = u_1(n_1,n_2),\\
&(L_{\updownarrow}u)_2(n_1,n_2) = \tfrac{1}{4}(u_2(n_1,n_2) + u_2(n_1,n_2-1) + u_2(n_1+1,n_2) + u_2(n_1+1,n_2-1)),\\
&(L_{\updownarrow}u)_3(n_1,n_2) = \tfrac{1}{2}(u_3(n_1,n_2) + u_3(n_1,n_2-1)),\\
&(L_{\updownarrow}u)_4(n_1,n_2) = \tfrac{1}{6}(u_4(n_1,n_2) + u_4(n_1,n_2-1) + u_4(n_1+1,n_2) + u_4(n_1+1,n_2-1) + u_4(n_1+2,n_2) + u_4(n_1+2,n_2-1)).\\
\\
&(L_{\leftrightarrow}u)_1(n_1,n_2) = \tfrac{1}{4}(u_1(n_1,n_2) + u_1(n_1-1,n_2) + u_1(n_1,n_2+1) + u_1(n_1-1,n_2+1)),\\
&(L_{\leftrightarrow}u)_2(n_1,n_2) = u_2(n_1,n_2),\\
&(L_{\leftrightarrow}u)_3(n_1,n_2) = \tfrac{1}{2}(u_3(n_1,n_2) + u_3(n_1-1,n_2)),\\
&(L_{\leftrightarrow}u)_4(n_1,n_2) = \tfrac{1}{2}(u_4(n_1,n_2) + u_4(n_1+1,n_2)).\\
\\
&(L_{\bullet}u)_1(n_1,n_2) = \tfrac{1}{2}(u_1(n_1,n_2) + u_1(n_1-1,n_2)),\\
&(L_{\bullet}u)_2(n_1,n_2) = \tfrac{1}{2}(u_2(n_1,n_2) + u_2(n_1,n_2-1)),\\
&(L_{\bullet}u)_3(n_1,n_2) = \tfrac{1}{4}(u_3(n_1,n_2) + u_3(n_1,n_2-1) + u_3(n_1-1,n_2) + u_3(n_1-1,n_2-1)),\\
&(L_{\bullet}u)_4(n_1,n_2) = \tfrac{1}{4}(u_4(n_1,n_2) + u_4(n_1+1,n_2) + u_4(n_1,n_2-1) + u_4(n_1+1,n_2-1)).
\end{aligned} \tag{11}
$$

Remark 2.2. In the above definition of operators, operator $L_{\updownarrow}$ operates on $u = (u_1, u_2, u_3, u_4)^T$, where $u_i \in \mathbb{R}^{N_1 \times N_2}$, $i = 1, 2, 3, 4$. Operator $L_{\updownarrow}$ use interpolation of some corresponding values on the neighbor pixels such that $(L_{\updownarrow}u)_1(n_1,n_2)$, $(L_{\updownarrow}u)_2(n_1,n_2)$, $(L_{\updownarrow}u)_3(n_1,n_2)$ and $(L_{\updownarrow}u)_4(n_1,n_2)$ belong to $A_{\updownarrow}$. Implementation of operators $L_{\leftrightarrow}, L_{+}$ and $L_{\bullet}$ are similar.

Now we propose the following new discrete total variation:

$$
TV_{new}(x) = \max_{u \in (\mathbb{R}^4)^{N_1 \times N_2}} \left\{ <\mathbb{D}x, u>: \ |L_{\updownarrow}u(n_1,n_2)| \leq 1, \ |L_{\leftrightarrow}u(n_1,n_2)| \leq 1, \ |L_{\bullet}u(n_1,n_2)| \leq 1, \ \forall (n_1,n_2) \in X \right\}, \tag{12}
$$

Note that for $\star = \updownarrow, \leftrightarrow, \bullet$

$$
|L_{\star}u(n_1,n_2)| = \sqrt{[(L_{\star}u)_1(n_1,n_2)]^2 + (L_{\star}u)_2(n_1,n_2)]^2 + (L_{\star}u)_3(n_1,n_2)]^2 + (L_{\star}u)_4(n_1,n_2)]^2}
$$

3. Fenchel-Rockafellar dual of the proposed regularization term

One of the best methods to solve mathematical image problems is primal-dual method. See some iterative methods to solve this kind of problems in [25, 28, 29]. In this section, some adjoint operators corresponding to the operators which are defined in the definition of the new regularization term (12) are given and consequently Fenchel-Rockafellar dual of (12) is found. Suppose $u \in (\mathbb{R}^3)^{N_1 \times N_2}$, then it is easy to see that $-\mathrm{div}u = \mathbb{D}^* u = u^*$, where

$$
\begin{gathered}
u^*(n_1,n_2) = [u_1(n_1-1,n_2) - u_1(n_1,n_2)] + [u_2(n_1-1,n_2-1) - u_2(n_1,n_2)] + \\
[u_3(n_1-1,n_2-1) - u_3(n_1,n_2)] + [u_3(n_1-1,n_2-1) - u_3(n_1,n_2)].
\end{gathered} \tag{13}
$$

Define

$$
K = \left\{ (u,s) \in (\mathbb{R}^4)^{N_1 \times N_2} \times (\mathbb{R})^{N_1 \times N_2} : s = -\mathrm{div}u, |L_{\star}u(n_1,n_2)| \leq 1, \star = \updownarrow, \leftrightarrow, \bullet, + \right\}, \tag{14}
$$

then obviously

$$
TV_{new}(x) = \max_{(u,s) \in (\mathbb{R}^4)^{N_1 \times N_2} \times (\mathbb{R})^{N_1 \times N_2}} \left\{ < x, s > - I_K\{(u,s)\} \right\}, \tag{15}
$$

where

$$
I_k\{t\} = \begin{cases} 0, & t \in K \\ \infty, & t \notin K \end{cases}.
$$

Now, we define operator L:

$$L = \begin{pmatrix} L_{\updownarrow} & 0 \\ L_{\leftrightarrow} & 0 \\ L_{\bullet} & 0 \\ \mathbb{D}^* & -1 \end{pmatrix}, \quad L\begin{pmatrix} u \in (\mathbb{R}^4)^{N_1\times N_2} \\ s \in \mathbb{R}^{N_1\times N_2} \end{pmatrix} = \begin{pmatrix} \bar{v}_{\updownarrow} \\ \bar{v}_{\leftrightarrow} \\ \bar{v}_{\bullet} \\ \bar{\alpha} \end{pmatrix} \in \begin{pmatrix} (\mathbb{R}^4)^{N_1\times N_2} \\ (\mathbb{R}^4)^{N_1\times N_2} \\ (\mathbb{R}^4)^{N_1\times N_2} \\ \mathbb{R}^{N_1\times N_2} \end{pmatrix} \tag{16}$$

In the sequel, we need dual definition of TV_{new}. Therefore, adjoint operators of $L_{\updownarrow}, L_{\leftrightarrow}, L_{\bullet}$ and L_{+} should be calculated. From the definition of adjoint operator of a linear operator, the following adjoint operators can be found:

Assume $v_{\updownarrow} = \begin{pmatrix} v^1_{\updownarrow} \\ v^2_{\updownarrow} \\ v^3_{\updownarrow} \\ v^4_{\updownarrow} \end{pmatrix} \in (\mathbb{R}^4)^{N_1\times N_2}$, $v_{\leftrightarrow} = \begin{pmatrix} v^1_{\leftrightarrow} \\ v^2_{\leftrightarrow} \\ v^3_{\leftrightarrow} \\ v^4_{\leftrightarrow} \end{pmatrix} \in (\mathbb{R}^4)^{N_1\times N_2}$ and $v_{\bullet} = \begin{pmatrix} v^1_{\bullet} \\ v^2_{\bullet} \\ v^3_{\bullet} \\ v^4_{\bullet} \end{pmatrix} \in (\mathbb{R}^4)^{N_1\times N_2}$ are dual variables and $v = \begin{pmatrix} v_{\updownarrow} \\ v_{\leftrightarrow} \\ v_{\bullet} \\ \alpha \end{pmatrix}$, then

$$L^*(v) = \begin{pmatrix} u_1^* \\ u_2^* \\ u_3^* \\ u_4^* \\ s^* \end{pmatrix} \in \begin{pmatrix} (\mathbb{R}^4)^{N_1\times N_2} \\ \mathbb{R}^{N_1\times N_2} \end{pmatrix}, \tag{17}$$

where

$$\begin{aligned}
&u_1^*(n_1,n_2) = v^1_{\updownarrow}(n_1,n_2) + \tfrac{1}{4}\left\{v^1_{\leftrightarrow}(n_1,n_2) + v^1_{\leftrightarrow}(n_1+1,n_2) + v^1_{\leftrightarrow}(n_1,n_2-1) + v^1_{\leftrightarrow}(n_1+1,n_2-1)\right\} + \\
&\quad \tfrac{1}{2}\left\{v^1_{\bullet}(n_1,n_2) + v^1_{\bullet}(n_1+1,n_2)\right\} + \{\alpha(n_1+1,n_2) - \alpha(n_1,n_2)\}, \\
&u_2^*(n_1,n_2) = \tfrac{1}{4}\left\{v^2_{\updownarrow}(n_1,n_2) + v^2_{\updownarrow}(n_1,n_2+1) + v^2_{\updownarrow}(n_1-1,n_2) + v^2_{\updownarrow}(n_1-1,n_2+1)\right\} + v^2_{\leftrightarrow}(n_1,n_2) + \\
&\quad \tfrac{1}{2}\left\{v^2_{\bullet}(n_1,n_2) + v^2_{\bullet}(n_1,n_2+1)\right\} + \{\alpha(n_1,n_2+1) - \alpha(n_1,n_2)\}, \\
&u_3^*(n_1,n_2) = \tfrac{1}{2}\left\{v^3_{\updownarrow}(n_1,n_2) + v^3_{\updownarrow}(n_1,n_2+1)\right\} + \tfrac{1}{2}\left\{v^3_{\leftrightarrow}(n_1,n_2) + v^3_{\leftrightarrow}(n_1+1,n_2)\right\} + \\
&\quad \tfrac{1}{4}\left\{v^3_{\bullet}(n_1,n_2) + v^3_{\bullet}(n_1,n_2+1) + v^3_{\bullet}(n_1+1,n_2) + v^3_{\bullet}(n_1+1,n_2+1)\right\} + \{\alpha(n_1+1,n_2+1) - \alpha(n_1,n_2)\}, \\
&u_4^*(n_1,n_2) = \tfrac{1}{6}\left\{v^4_{\updownarrow}(n_1,n_2) + v^4_{\updownarrow}(n_1,n_2+1) + v^4_{\updownarrow}(n_1-1,n_2) + v^4_{\updownarrow}(n_1-1,n_2+1) + v^4_{\updownarrow}(n_1-2,n_2) + v^4_{\updownarrow}(n_1-2,n_2+1)\right\} + \\
&\quad \tfrac{1}{2}\left\{v^4_{\leftrightarrow}(n_1,n_2) + v^4_{\leftrightarrow}(n_1-1,n_2)\right\} + \tfrac{1}{4}\left\{v^4_{\bullet}(n_1,n_2) + v^4_{\bullet}(n_1-1,n_2) + v^4_{\bullet}(n_1,n_2+1) + v^4_{\bullet}(n_1-1,n_2+1)\right\} + \\
&\quad \{\alpha(n_1+1,n_2+1) - \alpha(n_1,n_2)\}, \\
&s^* = -\alpha(n_1,n_2).
\end{aligned} \tag{18}$$

Now we need the following theorem. To find Fenchel-Rockafellar dual of the proposed regularization term:

Theorem 3.1. *(Fenchel Duality Theorem)[27]: Assume X, Y are real Banach spaces, $f : X \to]-\infty, +\infty]$ and $g : Y \to]-\infty, +\infty]$ are proper, convex and lower-semicontinuous functions and $A : X \to Y$ is a linear continuous operator, if there exists $x_0 \in X$ such that $f(x_0) < \infty$ and g is continuous at Ax_0, then*

$$\max\{-f(x) - g(Ax), x \in X\} = \min\{g^*(y^*) + f^*(-A^*y^*), y^* \in Y^*\} \tag{19}$$

Theorem 3.2. *TV_{new} (12)is equivalent to the following minimization problem:*

$$\begin{aligned} TV_{new}(x) = \min_{v_{\updownarrow}, v_{\leftrightarrow}, v_{\bullet}, \alpha} |v_{\updownarrow}| + |v_{\leftrightarrow}| + |v_{\bullet}| \\ s.t.\ \ L^* \begin{pmatrix} v_{\updownarrow} \\ v_{\leftrightarrow} \\ v_{\bullet} \\ \alpha \end{pmatrix} = \begin{pmatrix} 0 \\ 0 \\ 0 \\ 0 \\ x \end{pmatrix} \end{aligned} \tag{20}$$

4. Simulation Results

In this section, we evaluate our new proposed regularization method and compare it with the state-of-the-art for some mathematical image problems-namely denoising and resolution enhancement problems. Interested readers can get the codes from the following web address:

`https://github.com/Alirezahosseini1359/A-New-Total-Variational-Algorithm-for-Image-Processing-`
All experiments are performed using Matlab R2014a on a Windows 10 platform with an Intel(R) Core(TM) i5-4200U CPU 2.30GHz.
Consider the general problem:

$$\min_{x \in \mathbb{R}^{N_1 \times N_2}} F(x) + \lambda TV(x). \tag{21}$$

Optimization problem (21) is the general mathematical model for most of image problems. For example, for denoising problem, where $y \in \mathbb{R}^{N_1 \times N_2}$ is an noisy image $F(x) = \frac{1}{2}||x - y||^2$, for deconvolution problem, $F(x) = \frac{1}{2}||Ax - y||^2$, and for upscaling or resolution enhancement problem, $F(x) = I_{\{x|Ax=y\}}$ and $\lambda = 1$ (Note that in this case, problem (21) is equivalent to $\min_{x \in \mathbb{R}^{N_1 \times N_2}} \{TV(x) \ : \ Ax = y\}$). In the two latest problems, A is some special linear operator. From theorem 3.1, it is easy to see that problem (21) with $TV = TV_{new}$ is equivalent to the following problem:

$$(v^*_{\updownarrow}, v^*_{\leftrightarrow}, v^*_{\bullet}, \alpha^*) \in \arg\min \left\{ F(x) + \lambda\{|v_{\updownarrow}| + |v_{\leftrightarrow}| + |v_{\bullet}|\} : L^* \begin{pmatrix} v_{\updownarrow} \\ v_{\leftrightarrow} \\ v_{\bullet} \\ \alpha \end{pmatrix} = \begin{pmatrix} 0 \\ 0 \\ 0 \\ 0 \\ x \end{pmatrix} \right\}. \tag{22}$$

From (17) and (18), we get

$$L^* = \begin{pmatrix} L^*_{\updownarrow} & L^*_{\leftrightarrow} & L^*_{\bullet} & \mathbb{D} \\ 0 & 0 & 0 & -1 \end{pmatrix},$$

therefore, (22) is equivalent to

$$v^* = (x^*, v^*_{\updownarrow}, v^*_{\leftrightarrow}, v^*_{\bullet}) \in \arg\min \left\{ F(x) + \lambda\{|v_{\updownarrow}| + |v_{\leftrightarrow}| + |v_{\bullet}|\} : L^*_{\updownarrow}(v_{\updownarrow}) + L^*_{\leftrightarrow}(v_{\leftrightarrow}) + L^*_{\bullet}(v_{\bullet}) = \mathbb{D}x \right\}. \tag{23}$$

The dual optimization problem corresponding to problem (23) is as follows:

$$u^* = (u^*_1, \cdots, u^*_4) \in \arg\min \{F^*(-\mathbb{D}^*(u)) : ||(L_{\updownarrow}(u)\ L_{\leftrightarrow}(u)\ L_{\bullet}(u))|| \leq \lambda\}. \tag{24}$$

In numerical experiments below, to solve problem (22) and equivalently problem (21) with $TV = TV_{new}$, we use the over relaxed primal-dual algorithm which was proposed by Condat. See Algorithm 1 of [16]. The algorithm generally can be used to solve the following optimization problem:

$$\text{argmin}_{x \in \mathbb{R}^{N_1 \times N_2}, v \in \mathcal{F}} \{F(x) + G(v) : Cv + Dx = 0\}, \tag{25}$$

where C and D are linear operators. F and G are functions whose corresponding proximal operators have simple forms or can be calculated easily. In our case

$$v = \begin{pmatrix} v_{\updownarrow} \\ v_{\leftrightarrow} \\ v_{\bullet} \end{pmatrix},\ \mathcal{F} = \begin{pmatrix} (\mathbb{R}^4)^{N_1 \times N_2} \\ (\mathbb{R}^4)^{N_1 \times N_2} \\ (\mathbb{R}^4)^{N_1 \times N_2} \\ (\mathbb{R})^{N_1 \times N_2} \end{pmatrix},\ G(v) = \lambda\{|v_{\updownarrow}| + |v_{\leftrightarrow}| + |v_{\bullet}|\}.$$

Furthermore, operators D and C can be defined by:

$$Dx(n_1, n_2) = \mathbb{D}x(n_1, n_2), (n_1, n_2) \in X \Rightarrow Dx \in (\mathbb{R}^4)^{N_1 \times N_2}, C = (L^*_{\updownarrow}\ L^*_{\leftrightarrow}\ L^*_{\bullet}).$$

In the following numerical experiments, to solve problem (21), Algorithm 1 of [16] is applied for Condat's TV and Algorithm 3-1 of [25] is used for upwind TV. Moreover, split Bregman algorithm is employed for isotropic TV (TV), total Laplace model (TL), second order total generalized variation (TGV), total curvature (TC) and infimal-convolution (INFCON) model. For more details about these regularization functionals and split Bregman algorithm refer to [24]. Proximal operator associated to function $F \in \Gamma^0(X)$ (the set of all convex, proper and l.s.c functions on X) is the solution of the following problem:

$$\min_y \delta F(y) + \frac{1}{2}\|y - x\|^2.$$

If y^* is the solution of this problem, we write $prox_{\delta F}(x) = y^*$.

It is not difficult to see that in the following algorithm, $prox_{\alpha G}$ is

$$(prox_{\alpha G}(v))_c(n_1, n_2) = v_c(n_1, n_2) - \frac{v_c(n_1, n_2)}{\max(|v_c(n_1, n_2)/(\alpha\lambda), 1)}, (n_1, n_2) \in X, c \in \{\updownarrow, \leftrightarrow, \bullet\}.$$

4.1. Denoising Problem

Assume noisy image is denoted by y. Now, we are going to solve the problem (21) with $F(x) = \frac{1}{2}\|x - y\|^2$ for some test problems. For any numerical experiment, the noisy image is constructed from the clean image via corrupting it by additive white Gaussian noise of standard deviation 0.18. 500 iterations of Algorithm 1, for Condat's TV and proposed one, Algorithm 3-1 of [25] for upwind TV model and for other variational models split Bregman algorithms [24] are applied.

4.1.1. Comparison

Now, we consider denoising problem for `Cameraman`, `Lena` and `Goldhill` test images. A part of any image is applied for experiments (see Table 1).

`Cameraman`	`Lena`	`Goldhill`
	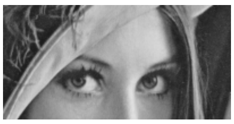	

Table 1: `Cameraman`, `Lena` and `Goldhill` test images for denoising problem.

4.2. Resolution enhancement

Resolution enhancement or upscaling problem can be considered as the inverse of downscaling problem. To downscale an image, usually the image is divided to some square blocks of the equal number of pixels. For any block, by averaging the intensity values of the pixels which are contained in it and assigning the obtained value to its intensity, the corresponding downscaled image will be constructed. Now, inversely suppose an $N \times N$ image y is given. The goal is constructing an $mN \times mN$, $m > 1$ image x such that y is downscale of x. Obviously, there is an infinite number of such images x. Let A be downscaling operator which maps an image to the image of its averages over 2×2 blocks ($m = 2$, that is, if x is an $2N\times2N$ image, then Ax is a downscaled $N\times N$ image). We define upscaling problem by $\min_{x\in\mathbb{R}^{N_1\times N_2}} F(x) + \lambda TV(x)$, where $\lambda = 1$ and $F(x) = I_{\{x\,:\,Ax=y\}}$. Because of convexity, this problem has a unique solution. For the following numerical experiments, any algorithms are applied with 500 iterations.

We solve upscaling problem of four test images: `Bike`, `Einstein`, `Fruits` and `Woman` (see Table 4).

	Parameters		Cameraman		Lena		Goldhill	
Model	Parameter 1 (C-L-G)	Parameter 2 (C-L-G)	$PSNR$	$SSIM$	$PSNR$	$SSIM$	$PSNR$	$SSIM$
Upwind	$\lambda = 0.19, 0.19, 0.16$	-	25.5374	0.7981	25.0323	0.6766	25.3598	0.5958
Isotropic	$\lambda = 0.15, 0.16, 0.16$	-	26.0904	0.7998	25.4277	0.6973	25.7910	0.6266
TC	$\mu_1 = 10, 10, 10$	$\mu_2 = \mu_1$	26.4009	**0.8463**	25.7086	0.7069	25.5197	0.6186
TL	$\alpha = 50, 50, 50$	$\theta = 10, 10, 10$	25.1981	0.7217	24.7515	0.6737	25.1173	0.6041
INFCON	$\alpha = 40, 40, 40$	$\beta = 2\alpha$	25.9966	0.8122	25.5663	0.7166	25.8533	0.6325
Condat	$\lambda = 0.14, 0.15, 0.14$	-	26.3477	0.8012	25.5906	0.7057	25.9012	0.6333
TGV	$\lambda_1 = 0.16, 0.15, 0.16$	$\lambda_2 = 2\lambda_1$	26.0896	0.8181	25.5547	0.7123	25.9012	0.6333
Proposed	$\lambda = 0.08, 0.08, 0.08$	-	**26.6866**	0.8350	**25.8106**	**0.7205**	**26.0667**	**0.6427**

Table 2: Denoising comparison: optimal parameters of different algorithms for different test images are used in comparison.

Reference	Noisy	TL	Isotropic(TV)	Upwind
				
TC	INFCON	Condat	TGV	Proposed
				

Table 3: Performance comparison of different methods for `Cameraman` denoising problem.

4.2.1. Comparison

In tables 5-6, reference, downscaled and upscaled images obtained by different variational models are illustrated (the upscaling problems are solved and the part of images corresponding to the red boxes from Table 4 are presented for comparison). For bike problem, it can be seen that, for the new proposed TV, the thickness of minute hand is narrower among other total variation models and its shape is closer to the reference image. For `Einstein` and `Woman` upscaling results, the edges of the upscaled images are smoother in the results which are obtained by the new proposed method (see the eyebrows, eyelids and eyelashes). The reconstruction of the edges in `Fruits` test problem shows that the edges are more smoothed in the proposed obtained results. The jagged edges in the downscaled image are notably smoothed, while in the other total variation models, large jagged edges still remain in the reconstructed images. Finally, PSNR and SSIM values show that the new method is more accurate in comparison with the state-of-the-art. Table 7 shows quantitative comparison of the different variational models and different sample images for upscaling problem.

5. Conclusion

In this paper, a new discrete total variation model was proposed to solve mathemathical image problems. The Fenchel-dual problem corresponding to the mathematical model of the new TV was constructed. We applied an

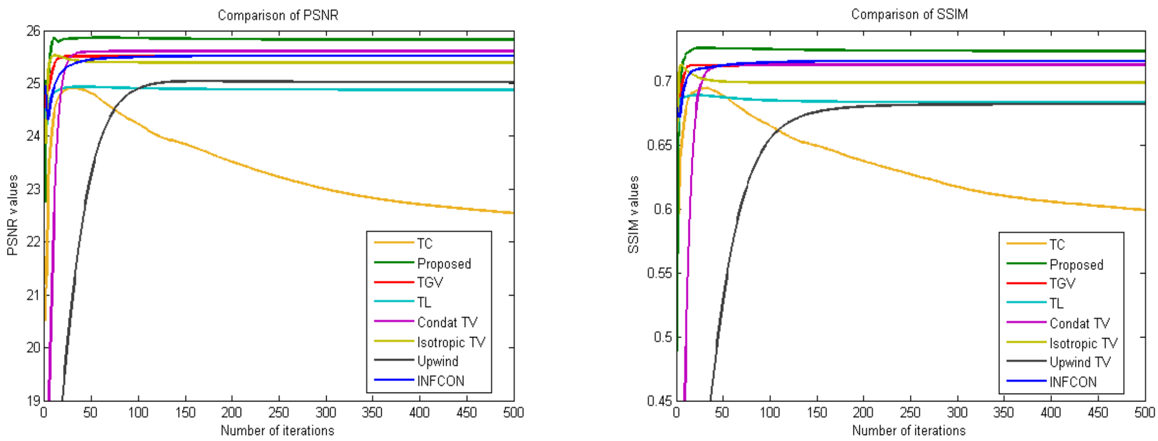

Figure 1: PSNR (left) and SSIM (right) values versus number of iterations for denoising `Lena` test image and different algorithms.

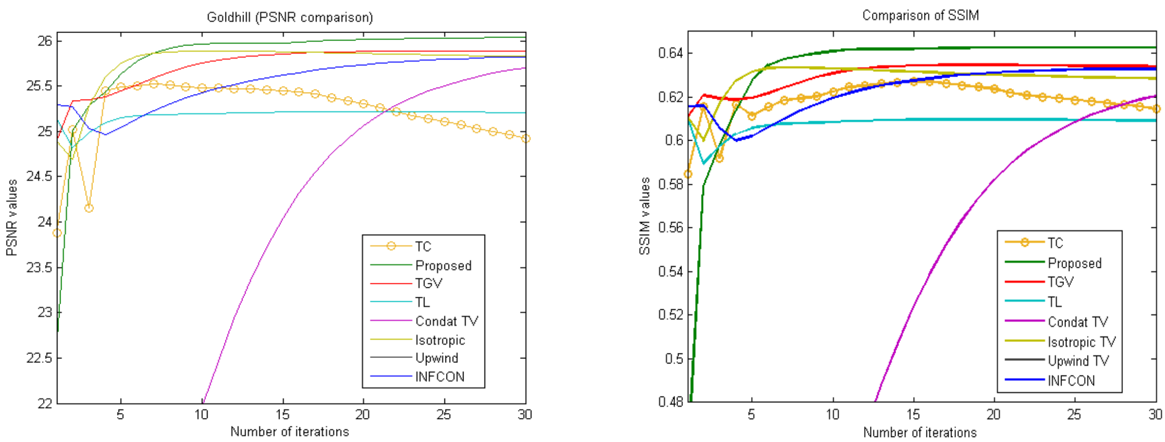

Figure 2: PSNR (left) and SSIM (right) values versus number of iterations for denoising `Goldhill` test image and different algorithms (the first 30 iterations are presented).

efficient primal-dual algorithm [16] in our numerical experiments. The results were compared with some other well-known TVs. The new proposed TV had the best results in reconstructing details of the images, smoothing and removing noise. Furthermore, for upscaling problem, four images were tested and compared with other TVs. The jagged parts of the downscaled images can be reconstructed by the proposed TV better than other familiar total variation models. Moreover, the new proposed TV has better performance in terms of smoothing edges, PSNR and SSIM values. In future works, we will try to use continuous total generalized variation model to construct the more efficient discrete model for image processing problems.

References

[1] Fan, M.Q., Wang, H.X.: An enhanced fragile watermarking scheme to digital image protection and self-recovery. Signal Processing: Image Communication. 66, 19-29 (2018).

[2] Leeuwen, T., Palenstijn, W.J., Aarle, W., Sijbers, J., Batenburg, K.J.: Easy implementation of advanced tomography algorithms using the ASTRA toolbox with Spot operators. Numer. Alg. 71, 673-697 (2015).

[3] Haider, M., Uhlemann, S., Schwan, E., Rose, H., Kabius, B., Urban, K.: Electron microscopy image enhanced. Nature. 392, 678-669 (1998).

[4] Shibata, N., Seki, T., Sanchez-Santolino, G., Findlay, S.D., Kohno, Y., Matsumoto, T., Ishikawa, R., Ikuhara, Y.: Electric field imaging of single atoms. Nature Communications. doi:10.1038/ncomms15631.

[5] Sadasivan, A.K., Senthilkumar, T.: Automatic Character Recognition in Complex Images. Procedia Engineering. 30, 218-225 (2012).

[6] Allison, D.B., Cui, X., Page, G.P., Sabripour, M.: Microarray data analysis: from disarray to consolidation and consensus. Nature Reviews

Bike	Einstein	Fruits	Woman
	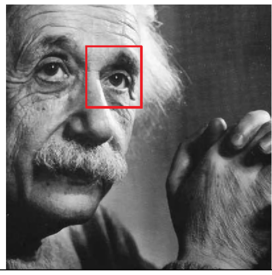	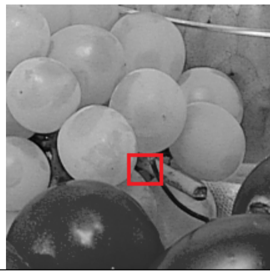	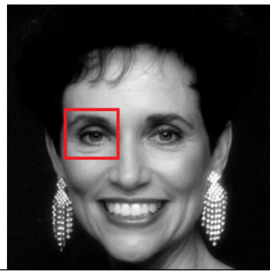

Table 4: `Bike`, `Einstein`, `Fruits` and `Woman` test images for upscaling.

Reference	Downscaled	Upwind
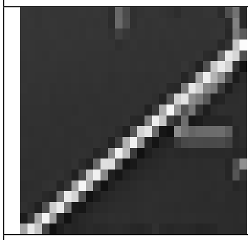	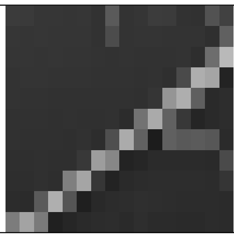	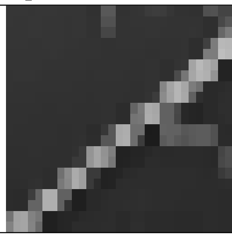
Condat	TGV	Proposed
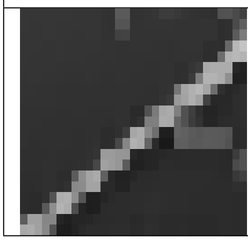	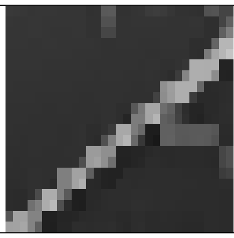	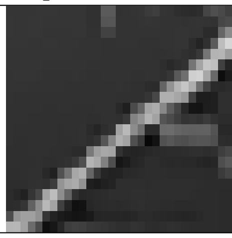

Table 5: Performance comparison of different methods for `Bike` upscaling problem.

Genetics. 7, 55-65 (2006).

[7] Pages, R., Berjon, D., Moran, F.: Automatic system for virtual human reconstruction with 3D mesh multi-texturing and facial enhancement. Signal Processing: Image Communication. 28, 1089-1099 (2013).

[8] Ringh, A., Karisson, J., Lindquist, A.: Multidimensional rational covariance extension with applications to spectral estimation and image compression. SIAM Journal on Control and Optimization. 54, 1950-1982 (2016).

[9] Maecca, R., Queau, Y., Logothetis, F., Cipolla, R.: A Single-Lobe Photometric Stereo Approach for Heterogeneous Material. SIAM Journal on Imaging Sciences. 9, 1858-1888 (2016).

[10] J. N. Reddy, Introductory Functional Analysis With Applications to Boundary Value Problems and Finite Elements, Springer-Verlag New York, Volume 27, 1988.

[11] Rudin, L., Osher, S., Fatemi, E.: Nonlinear total variation based noise removal algorithms. Phys. D. 60, 259-268 (1992).

[12] Chambolle, A., Pock, T.: A first-order primal-dual algorithm for convex problems with applications to imaging. J. Math. Imaging Vision. 40, 120-145 (2011).

[13] Chambolle, A., Cremers, D., Pock, T.: A convex approach to minimal partitions. SIAM J. Imaging Sci. 5, 1113-1158 (2012).

[14] Chambolle, A., Levine, S.E., Lucier, B. J.: An upwind finite-difference method for total variation based image smoothing. SIAM J. Imaging Sci. 4, 277-299 (2011).

[15] Alter, F., Caselles, V., Chambolle, A.: Evolution of characteristic functions of convex sets in the plane by the minimizing total variation flow. Interfaces Free Bound. 7, 29-53 (2005).

[16] Condat, L., Discrete Total Variation: New Definition and Minimization. SIAM J. Imaging Sci. 10, 1258-1290 (2017).

[17] Bredies, K., Kunisch, K., Pock, T., Total generalized variation. SIAM J. Imaging Sci. 3, 492-526 (2010)

[18] You, YL., Kaveh, M., Fourth-order partial differential equations for noise removal. IEEE Transactions on Image Processing 9(10), 1723-1730 (2000).

[19] Zhu, W., Chan, TF., Image denoising using mean curvature of image surface. SIAM Journal on Imaging Sciences 5(1), 1-32 (2012).

[20] Chambolle, A., Lions, PL., Image recovery via total variation minimization and related problems. Numerische Mathematik 76(2), 167-188

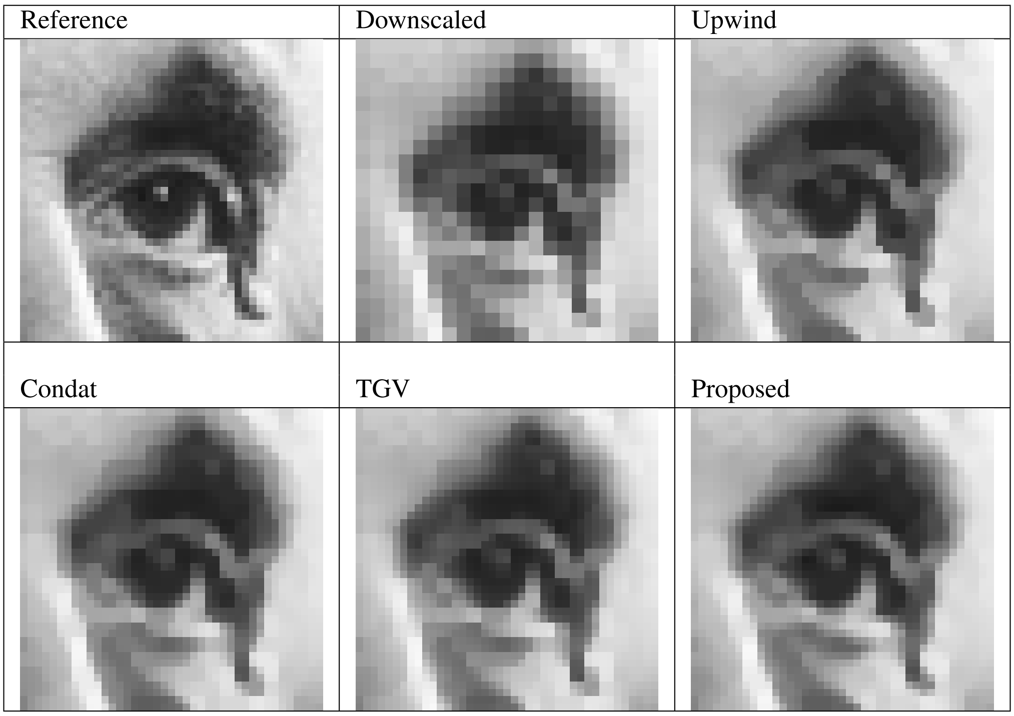

Table 6: Performance comparison of different methods for `Einstein` upscaling problem.

	`Bike`		`Einstein`		`Fruits`		`Woman`	
Model	$PSNR$	$SSIM$	$PSNR$	$SSIM$	$PSNR$	$SSIM$	$PSNR$	$SSIM$
Upwind	25.0860	0.8937	32.2675	0.8997	32.3958	0.9086	32.4535	0.9567
Isotropic	25.0141	0.8917	32.2199	0.8994	32.0625	0.9063	32.3851	0.9554
Condat	25.3213	0.8977	32.4448	0.9025	32.6442	0.9118	32.5317	0.9573
TGV	25.0695	0.8930	32.3734	0.9013	32.1229	0.9077	32.5635	0.9587
Proposed	**25.4853**	**0.9010**	**32.7567**	**0.9062**	**33.1790**	**0.9161**	**33.6370**	**0.9618**

Table 7: Upscaling comparison for different algorithms and different test images.

(1997).
[21] Getreuer, P., Rudin-Osher-Fatemi total variation denoising using split Bregman. Image Processing On Line 2, 74-95 (2012).
[22] Duan, J., Qiu, Z., Lu, W., Wang, G., Pan, Z., Bai, L., An edge-weighted second order variational model for image decomposition. Digital Signal Processing 49, 162-181 (2016).
[23] Duan, J., Lu, W., Tench, C., Gottlob, I., Proudlock, F., Samani, N., Bai, L., Denoising optical coherence tomography using second order total generalized variation decomposition. Biomedical Signal Processing and Control 24, 120-127 (2016).
[24] Lu, W., Duan, J., Qiu, Z., Pan, Z., Liu, R. W., Bai, L., : Implementation of high-order variational models made easy for image processing, Mathematical Methods in Applied Sciences DOI: 10.1002/mma.3858.
[25] Condat, L.: A primal-dual splitting method for convex optimization involving Lipschitzian, proximable and linear composite terms, J. Optim. Theory Appl. 158, 460-479 (2013).
[26] Abergel, R., Moisan, L.: The Shannon total variation. J. Math Imaging Vis. DOI 10.1007/s10851-017-0733-5.
[27] Bauschke, H.H., Combettes, P.L.: Convex Analysis and Monotone Operator Theory in Hilbert Spaces. Springer. New York (2011).
[28] Condat, L.: A generic proximal algorithm for convex optimization-Application to total variation minimization. IEEE Signal Processing Lett. 21, 1054-1057 (2014).
[29] Combettes, P.L., Condat, L., Pesquet, J.C., Vũ, B.C.: A forward-backward view of some primal-dual optimization methods in image recovery. In Proc. of IEEE ICIP. Paris. France (2014).